



CD8⁺ T-cell exhaustion in the tumor microenvironment of head and neck squamous cell carcinoma determines poor prognosis

Yijian Zhang^{1#}, Li Li^{2#}, Wenjie Zheng³, Lei Zhang¹, Ninghua Yao^{2^}

¹Department of Otolaryngology-Head and Neck Surgery, Affiliated Hospital of Jiangnan University, Wuxi, China; ²Department of Oncology, Affiliated Hospital of Nantong University, Nantong, China; ³Research Center of Clinical Medicine, Affiliated Hospital of Nantong University, Nantong, China

Contributions: (I) Conception and design: Y Zhang, N Yao; (II) Administrative support: L Zhang, W Zheng; (III) Provision of study materials or patients: L Li; (IV) Collection and assembly of data: Y Zhang, N Yao; (V) Data analysis and interpretation: N Yao; (VI) Manuscript writing: All authors; (VII) Final approval of manuscript: All authors.

[#]These authors contributed equally to this work.

Correspondence to: Dr. Ninghua Yao. Department of Oncology, Affiliated Hospital of Nantong University, Nantong 226001, China. Email: yaonh2009@163.com.

Background: The occurrence of head and neck squamous cell carcinoma (HNSCC) is closely related to the immune system. The integration of traditional treatment methods and immunotherapy will be the future development direction of cancer treatment. But immunotherapy also has its limitations: a lot of basic research is going on, but the translation from basic to clinical is still not enough, and there are still few drugs approved for use. This study aimed to explore the clinical significance of the tumor immune microenvironment in HNSCC.

Methods: Six clinically obtained postoperative cases were analyzed using multiplex immunohistochemistry (mIHC) to observe the tumor immune microenvironment and analyze infiltrating immune cells. Correlations between infiltrating immune cells from The Cancer Genome Atlas (TCGA) database and clinicopathological features of 510 HNSCC patients were then analyzed. Kaplan-Meier survival analysis was used to detect the relationship between the expression of different immune cells and the prognosis of HNSCC patients, and univariate and multivariate Cox regression analyses were used to analyze the prognostic factors associated with HNSCC patients. We validated the prognostic and predictive accuracy based on the expression of CD8⁺ T-cells in an independent group of 510 patients.

Results: We detected infiltration of CD8⁺ T cells, NK cells, and macrophages in patients with laryngeal squamous cell carcinoma by multiplex immunofluorescence. The infiltration of the three types of immune cells in the tumor stroma was significantly higher than in the tumor parenchyma. Our results also showed the infiltration of CD8⁺ T cells was associated with prognosis, and the COX regression model showed CD8⁺ T cells were an independent prognostic factor in HNSCC patients. The higher density of infiltrating CD8⁺ T cells had the better prognosis. In addition, we developed a nomogram for clinical use that integrated the CD8⁺ T-cells-based classifier and three clinicopathological risk factors to predict the prognosis of HNSCC patients.

Conclusions: CD8⁺ T-cell exhaustion in the tumor microenvironment of HNSCC determines poor prognosis and can be combined with the tumor stage to improve the accuracy of prognosis assessment in HNSCC patients.

Keywords: CD8⁺ T cell; head and neck squamous cell carcinoma (HNSCC); tumor microenvironment; The Cancer Genome Atlas (TCGA); immune infiltrates

Submitted Jan 25, 2022. Accepted for publication Mar 14, 2022.

doi: 10.21037/atm-22-867

View this article at: <https://dx.doi.org/10.21037/atm-22-867>

[^] ORCID: 0000-0002-7607-2516

Introduction

Head and neck squamous cell carcinoma (HNSCC) is the sixth most common cancer globally, with about 600,000 newly diagnosed cases every year (1). Most patients present with locally advanced disease with apparent lymph node metastasis. Whilst significant progress has been made in the diagnosis and treatment of HNSCC in the past few decades, and the disease control rate and survival rate of patients have greatly improved, only 50% of patients receive radical treatment, and the recurrence and metastasis rates are 40% and 60%, respectively (2,3). Immunotherapy has developed rapidly in recent years, and various drugs have been approved for the treatment of different tumors. Immune checkpoint PD-1 inhibitors represented by nivolumab and pembrolizumab can effectively improve the survival prognosis of patients with recurrent/metastatic HNSCC who have failed platinum therapy and have good safety. An ideal biomarker has three properties: diagnosis, prognosis and prediction. A biomarker may have both prognostic and predictive roles. At present, there are not many biomarkers for HNSCC that have been identified for clinical use, and they are mainly related to the causative virus of the tumor. For example, EBV and HPV are the established prognostic biomarkers for head and neck squamous cell carcinoma, but they do not have both definite predictive functions and cannot be used to meet clinical needs. Therefore, more prognostic markers are sought to precisely find the target of tumor therapy.

Most HNSCC has obvious immune infiltration, and the interaction between immune cells, tumor cells, and their products in the tumor immune microenvironment will limit the efficacy of immunotherapy (4). In addition to inhibiting antigen expression, tumor cells also inhibit the immune response by releasing certain immunosuppressive cells or chemical factors into the immune microenvironment. HNSCC cells can secrete TGF- β and IL-10, inhibiting T cell proliferation and cell killing function (5). In addition, they can also release chemical factors such as CCL5 and CXCL10 to induce many immunosuppressive hematopoietic cells into the immune microenvironment (6). de Ruiter *et al.* (7) analyzed the efficacy of the prognosis of HNSCC patients and found specific immune cell types such as CD3⁺ and CD8⁺ were positively correlated with it. Another prognostic analysis study on the efficacy of PD-1 treatment showed higher CD8⁺ T cell infiltration indicated a better prognosis (8), and a 2015 meta-analysis found high CD8⁺ T cells were significantly associated with longer OS

in tumor parenchyma and stroma. NK cells, which destroy cancer cells and initiate immune responses by secreting immunoregulatory cytokines, are also associated with a better prognosis (7).

In blood circulation, NK cells can effectively kill tumor cells and can block tumor metastasis through blood circulation. Patients with HNSC have increased infiltration of NK cells in the tumor tissue, often showing a favorable prognosis (9,10). Other studies have also found that the tumor immune microenvironment is beneficial to myeloid-derived suppressor cells (MDSCs), the expression of IL-1 and IL-6 in cancer cells, M2-polarized tumor-associated macrophages (TAMs), and N2 tumor-associated macrophages. Tumor-associated neutrophils (TANs) can inhibit the efficacy of ICI (11,12), while TAMs infiltrate the tumor microenvironment and play a role in tumor initiation, progression, metastasis, and angiogenesis. TAMs are classified into M1 and M2 types according to biological properties and surface markers. The M1 type is mainly involved in the inflammatory response and anti-tumor immune process, while the M2 type promotes tumor and immunosuppression. In 13 studies that included a total of 2,218 patients with HGSOC receiving platinum-based chemotherapy, the studies have confirmed that M1 macrophages are associated with good overall survival (OS), while M2 predicts poor OS (13).

While the traditional immunohistochemical diaminobenzidine (DAB) chromogenic method detects single-stained proteins when localizing the expression of the double-stained protein, multiplex immunofluorescence staining technology detects multiple biomarkers. While this technology saves pathological materials and verifies the interaction between different proteins (14), in some cases there are few specimens, including endoscopic specimens, and needle biopsy specimens, which leads to insufficient samples in the detection of polyprotein staining (15). Using the principle of antigen-antibody specific binding, multiple immunofluorescence staining technologies can visualize, quantify, characterize, and co-localize various proteins in tumor cells, providing the necessary means for tumor cell research (16,17).

In this experiment, the number and spatial distribution of immune infiltrating cells in the tumor parenchyma and stroma were evaluated by observing the immune microenvironment of HNSCC by multi-label immunofluorescence technology, and the results showed the immune infiltrating cells in the tumor parenchyma in HNSCC were higher than those in the stroma. At the same time, we found the infiltration of CD8⁺

Table 1 Baseline data of 6 patients with laryngeal squamous cell carcinoma

| ID | Age, years | Gender | T | N | Stage | Differentiation |
|-----------|------------|--------|---|---|-------|-----------------|
| Patient 1 | 56 | Male | 3 | 0 | III | High |
| Patient 2 | 59 | Male | 4 | 2 | IV | Moderate |
| Patient 3 | 59 | Male | 3 | 2 | IV | Moderate |
| Patient 4 | 48 | Male | 3 | 0 | III | High |
| Patient 5 | 76 | Male | 3 | 0 | III | High-moderate |
| Patient 6 | 62 | Male | 2 | 0 | II | Moderate-low |

T cells was associated with prognosis and was an independent prognostic factor through the TCGA database, and the higher the infiltrating number of CD8⁺ T cells, the better the patient's prognosis. We present the following article in accordance with the TRIPOD reporting checklist (available at <https://atm.amegroups.com/article/view/10.21037/atm-22-867/rc>).

Methods

Patients

Six patients were retrospectively screened for multiplex immunohistochemical (mIHC) analysis among all patients undergoing radical laryngectomy for laryngeal cancer at the Affiliated Hospital of Jiangnan University. The inclusion criteria included a pathological diagnosis of squamous cell carcinoma and a clear clinicopathological stage (*Table 1*). All procedures performed in this study involving human participants were in accordance with the Declaration of Helsinki (as revised in 2013). Informed consent was obtained from the six patients, and the Ethics Committee of Affiliated Hospital of Jiangnan University approved the study protocol (No. LS2021073). Clinicopathological classification and staging were performed using the American Joint Committee on Cancer criteria. In addition, data of 510 patients with HNSCC with precise clinicopathological staging and follow-up information was obtained in The Cancer Genome Atlas (TCGA, <https://portal.gdc.cancer.gov/>) database (*Table 2*). All raw gene expression and clinical data were processed by R language (R version 4.1.2).

Multiplex immunohistochemistry

All FFPE slides were dewaxed, hydrated, antigen-repaired, and stained on a Leica Bond III automated

Table 2 Baseline data of 510 HNSCC patients obtained from the TCGA database

| Characteristics | Overall |
|--------------------------|--------------|
| Total | 510 |
| Sex, n (%) | |
| Female | 132 (25.9) |
| Male | 378 (74.1) |
| T, n (%) | |
| T1 | 35 (6.9) |
| T2 | 148 (29) |
| T3 | 135 (26.5) |
| T4 | 181 (35.5) |
| TX | 11 (2.2) |
| N, n (%) | |
| N0 | 241 (47.3) |
| N1 | 82 (16.1) |
| N2 | 160 (31.4) |
| N3 | 9 (1.8) |
| NX | 18 (3.5) |
| M, n (%) | |
| M0 | 485 (95.1) |
| M1 | 6 (1.2) |
| MX | 19 (3.7) |
| Stage, n (%) | |
| I | 27 (5.3) |
| II | 81 (15.9) |
| III | 94 (18.4) |
| IV | 308 (60.4) |
| Grade, n (%) | |
| G1 | 61 (12) |
| G2 | 297 (58.2) |
| G3 | 123 (24.1) |
| G4 | 7 (1.4) |
| GX | 22 (4.3) |
| Age, years, median [IQR] | 60.5 [53–68] |

TCGA, The Cancer Genome Atlas; HNSCC, head and neck squamous cell carcinoma; T, tumor; N, node; M, metastasis; IQR, interquartile range.

immunohistochemical staining machine. The antigen repair conditions were as follows: Boiling at 100 °C for 20 min in ER2 antigen repair solution, incubation at room temperature for 15 min in 3% H₂O₂ to eliminate the endogenous peroxidase activity, and closure for 10 min by adding the closure solution. CD8 primary antibody (antibody dilution/closure solution diluted at 1:300) was added for 30 min at room temperature, the secondary antibody for 10 min (Leica goat anti-rabbit poly-HRP), and TSA fluorescent dye (1:100) for 10 min. Slides were washed with 1× Tris-buffered saline-Tween 20 (TBST) buffer for 3–5 min between each step. To stain six markers in a single slide, five rounds of the above staining procedure were performed using the indicated primary antibody (CD68, 1:400; HLA-DR, 1:1,000; CD56, 1:100; PanCK, 1:400; S100, 1:400) and the matching TSA fluorescent dye pair. After five rounds, sample cell DNA was stained with 4',6-diamidino-2-phenylindole (DAPI) (1:10) for 10 min, and the slides were finally sealed with an anti-fluorescence quencher. All slides were photographed and analyzed using Panoramic/HALO quantitative histopathological scan analysis software for multiple typical fields of view. The number of each type of positive cells was output according to the tumor parenchyma and mesenchymal area, respectively, and the cell density and positive rate within the corresponding area were calculated, where the number of positive cells in the tumor parenchyma or mesenchymal area/tissue area of the tumor parenchyma or mesenchymal area was defined as cell density. The number of positive cells in the tumor parenchyma or mesenchymal area/total number of cells in the tumor parenchyma or mesenchymal area was defined as cell positivity rate. Necrotic cells and tissue areas were not counted in the analysis.

Identification and construction of prognosis-related immune cell subpopulations

Univariate and multivariate analysis screened prognostic factors from different clinical parameters and immune cell subpopulations, and Kaplan-Meier survival analysis was used to detect the relationship between the expression of various immune cells and the prognosis of HNSCC patients.

Construction and validation of prognosis-related immune cell subpopulations

A prognostic nomogram was constructed to evaluate the probability of 4- and 8-year survival for HNSCC patients

(n=510), including age, gender, stage, B cell, and CD8⁺ T cell. Calibration curves were then performed to evaluate the validity of the model. To assess the predictive accuracy of the prognosis-related immune cell subpopulations, receiver operating characteristic (ROC) curves for 4- and 8-year survival were constructed, and the area under the curve (AUC) values were also determined.

Statistical analysis

Wilcoxon and Kruskal-Wallis tests were used to compare continuous variables, and categorical variables were analyzed using the chi-square test. Kaplan-Meier analysis with the log-rank test were used to compare OS between different groups. Univariate and multivariate Cox regression analyses were implemented to identify prognostic predictors, and Cox regression coefficients were used to generate nomograms. Calibration plots were generated to explore the performance characteristics of the nomograms. The x-axis represents the prediction calculated using the nomogram, and the y-axis represents the actual freedom from cancer recurrence. All statistical analyses were performed with R software version 4.0.1 and P<0.05 was considered statistically significant.

Results

Characterization of tumor immune infiltrates in HNSCC

Detection of tumor immune cell infiltration in six patients with squamous cell carcinoma of the larynx was performed using mIHC, and the presence of infiltration of CD8⁺ T cells, natural killer cells (NK cell), and macrophages is shown in *Figure 1A,1B*. To clarify whether significant immune cell infiltration was present in the parenchyma or the stroma, cell counts were performed in mIHC sections of the six samples, and a heatmap shows the results of the infiltration of the three immune cell subpopulations (*Figure 1C*), while *Figure 1D-1I* shows the infiltration in a box plot format. Mean and standard deviation of CD8⁺ T cells density in tumor parenchyma and stroma were 306.712±208.014 and 593.102±452.333, mean and standard deviation of M1 cells density in tumor parenchyma and stroma were 146.59±81.90 and 548.07±200.14, mean and standard deviation of M2 cells density in tumor parenchyma and stroma were 146.05±112.79 and 571.88±322.911, mean and standard deviation of NK CD56 bright cells density in tumor parenchyma and stroma were 6.64±2.31 and 31.30±14.26,

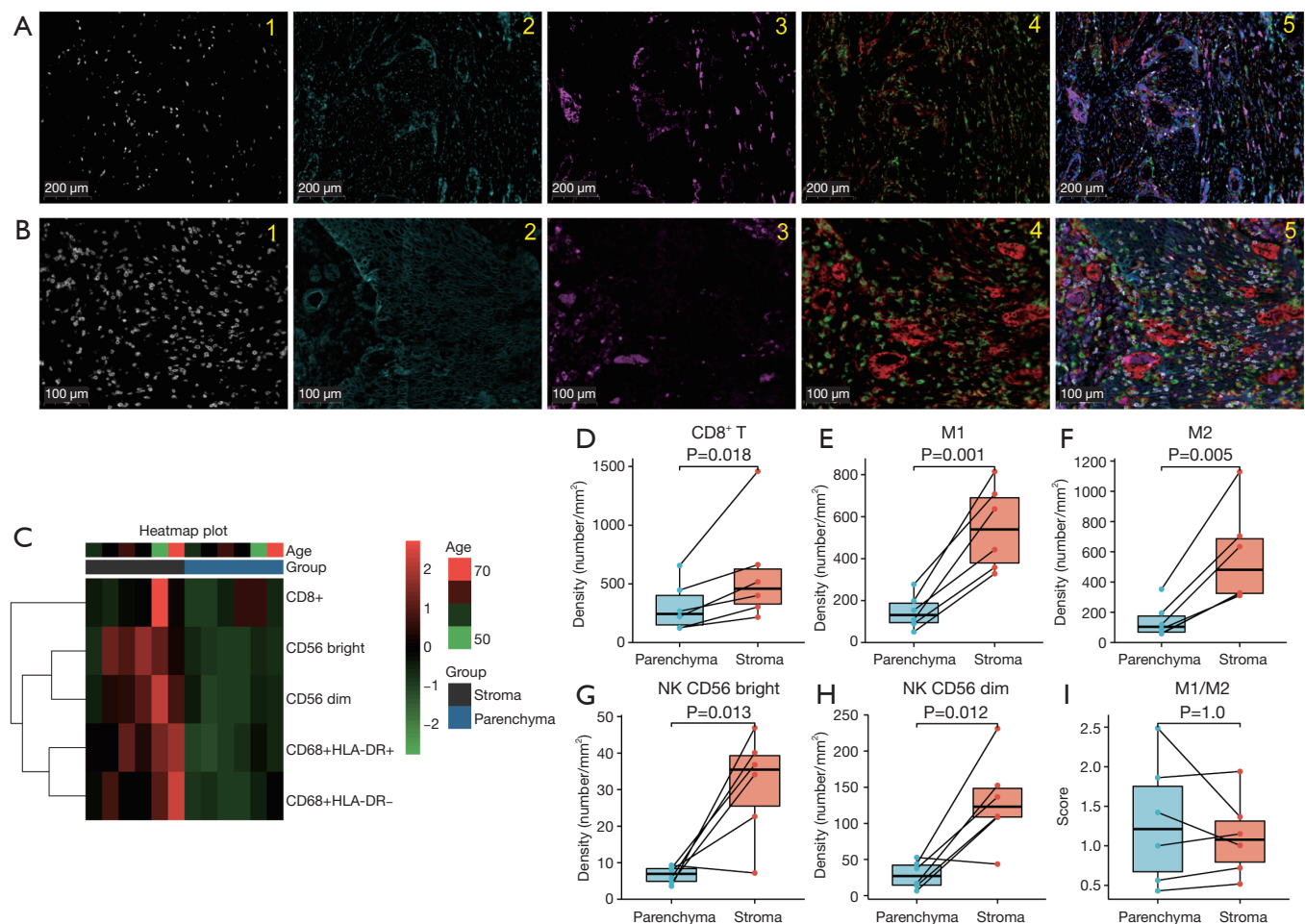


Figure 1 Different tumor immune cell infiltration status in HNSCC patients. (A,B) Typical high-resolution images of mIHC from two random samples. Different colours represent different immune cell subpopulations. white, CD8; cyan, PanCK; purple, CD56; green, CD68; red, HLA-DR. (C) Heatmap of the infiltration of immune cells in the parenchyma and stroma. (D-I) The box diagram shows the infiltration of different immune cell subtypes in the parenchyma and stroma. HNSCC, head and neck squamous cell carcinoma; mIHC, multiplexed immunohistochemistry; M, macrophage; NK cell, natural killer cells.

mean and standard deviation of NK CD56 dim cells density in tumor parenchyma and stroma were 28.59 ± 18.63 and 130.33 ± 61.83 . The results showed all three immune cells were significantly infiltrated in the stroma in different immune cell subpopulations, except for macrophages in the process of polarization, where there was no difference in the infiltration in the parenchyma or the stroma.

Correlation between variety of tumor immune cell infiltration and prognosis

A heatmap for the association between different immune cell subpopulations and clinicopathological features is

shown in *Figure 2A*. In addition, Kaplan-Meier survival curve analysis showed that patients with high expression of endothelial cells, CD8⁺ T cells, and B cells had a better prognosis ($P < 0.001$), a low CD4⁺ T cell expression suggested a better prognosis ($P = 0.04$), and no significant correlation with prognosis was found in NK cells, macrophages, and cancer-associated fibroblasts (*Figure 2B*). Combined with our mIHC results, it can be inferred that CD8⁺ T cells and B cells are independent prognostic factors for HNSCC patients, although the role of the latter requires further validation.

Univariate and multivariate COX regression analyses were used to identify prognosis-related immune cell subpopulations

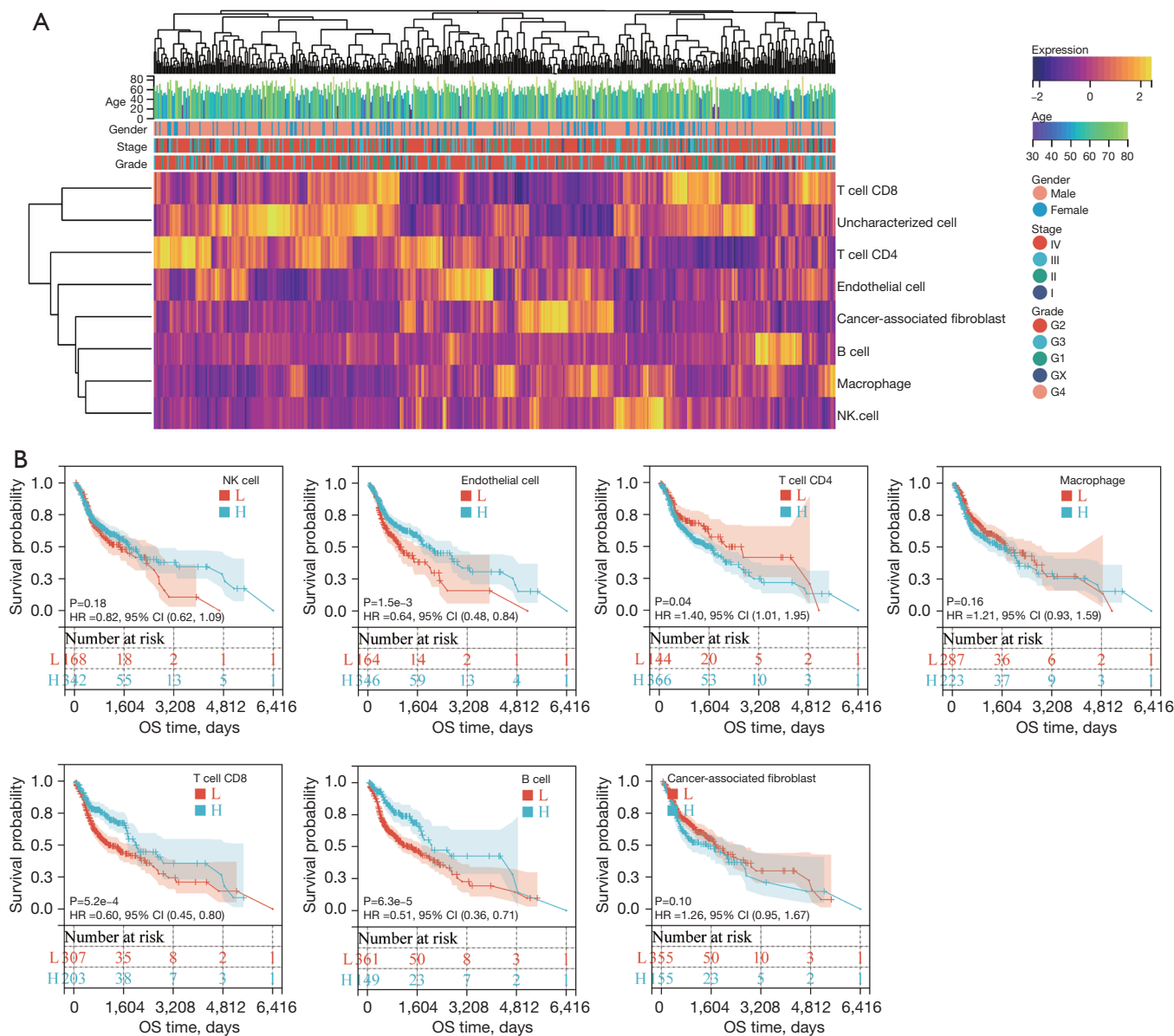


Figure 2 Relationship between different immune cell subpopulations and the prognosis of HNSCC patients. (A) Heatmap of the relationship between immune cell subpopulations and clinical characteristics; (B) OS of differential expression of NK cells, endothelial cells, CD4 T cells, macrophages, CD8 T cells, B cells, and cancer-associated fibroblast in HNSCC patients. HNSCC, head and neck squamous cell carcinoma; OS, overall survival; NK cell, natural killer cells.

in different tumor-infiltrating immune cells (Table 3), and both showed age, stage IV, B cells, and CD8⁺ T cells were significantly associated with the prognosis of HNSCC.

Nomograms to predict prognosis of OS in HNSCC

A prognostic nomogram including the prognosis-related immune cell subpopulations and clinical characteristics was

used to evaluate the accuracy and clinical applicability of the prognostic model (Figure 3A). The overall C-index of the model was 0.63 (95% CI: 0.58–0.67, P=6.4e-09). The time-dependent ROC curve demonstrated that the AUC value for 4- and 8-year of the prognosis-related immune cell subpopulations in predicting the prognosis of HNSCC was 0.64 and 0.73, respectively (Figure 3B), and calibration curves formalized the reliability of the model (Figure 3C).

Table 3 Univariate and multivariate Cox analysis of HNSCC clinicopathological factors

| Characteristics | Total (N) | Univariate analysis | | Multivariate analysis | |
|------------------------------|-----------|---------------------------------|---------|-----------------------|---------|
| | | Hazard ratio (95% CI) | P value | Hazard ratio (95% CI) | P value |
| Age | 510 | 1.018 (1.005–1.031) | 0.005 | 1.020 (1.007–1.033) | 0.003 |
| Stage | 510 | | | | |
| I | 27 | Reference | | | |
| II | 81 | 2.157 (0.760–6.120) | 0.148 | 2.141 (0.754–6.078) | 0.153 |
| III | 94 | 2.442 (0.866–6.889) | 0.092 | 2.652 (0.940–7.481) | 0.065 |
| IV | 308 | 3.405 (1.260–9.197) | 0.016 | 3.498 (1.294–9.459) | 0.014 |
| Grade | 510 | | | | |
| G2 | 297 | Reference | | | |
| G3 | 123 | 0.828 (0.599–1.145) | 0.254 | | |
| G1 | 61 | 0.613 (0.390–0.964) | 0.034 | | |
| GX | 22 | 0.600 (0.279–1.290) | 0.191 | | |
| G4 | 7 | 0.000 (0.000–Inf) | 0.992 | | |
| B cell | 510 | 0.000 (0.000–0.003) | 0.005 | 0.000 (0.000–0.017) | 0.010 |
| Cancer-associated fibroblast | 510 | 0.841 (0.358–1.973) | 0.690 | | |
| T cell CD4 | 510 | 2.688 (0.155–46.673) | 0.497 | | |
| T cell CD8 | 510 | 0.000 (0.000–0.011) | 0.005 | 0.000 (0.000–0.366) | 0.032 |
| Endothelial cell | 510 | 0.000 (0.000–72.063) | 0.209 | | |
| Macrophage | 510 | 154.583 (0.000–84,002,295.704) | 0.454 | | |
| NK cell | 510 | 0.051 (0.000–932,749,993,272.6) | 0.848 | | |

Univariate variables with $P < 0.05$ were chosen for the multivariate analysis. COX, proportional hazards model; HNSCC, head and neck squamous cell carcinoma; CI, confidence interval; NK cell, natural killer cells.

Discussion

HNSCCs are common malignant tumors globally, with a high metastasis rate and low survival rate (18). Previous study has found HNSCC exhibits immunosuppressive features (8), the role of tumor immune infiltrating cells in the immune microenvironment requires further study.

The immune system plays an important role in the body's anti-tumor process, especially the adaptive immune system, and previous studies have shown this can monitor tumors and eliminate new tumors. $CD8^+$ T lymphocytes in the tumor immune microenvironment are an important part of a tumor's adaptive immune system and are involved in antigen presentation, tumor cell cycle inhibition, apoptosis, angiogenesis, and the induction of macrophage killing activity. Tumor infiltrating lymphocytes (TILs) participate in the formation of the tumor microenvironment, reflect

the local immune response of the tumor, and play a key role in controlling the development of tumors (19). Rosenberg *et al.* isolated and reported TILs for the first time in 1986, and IL-2 stimulation *in vitro* can effectively enhance their immune activity (20), resulting in a significant tumor-killing effect. Tumor infiltrating $CD8^+$ T cells are an important part of TILs. $CD8^+$ T cells mediate the type 1 immune response, enhancing the aggregation of $CD8^+$ and $CD4^+$ T cells, and promoting their anti-tumor effects (21). A 2015 meta-analysis that included 6,543 patients from 18 articles found that high levels of CD8 were significantly associated with longer OS (22). However, the number of infiltrating lymphocytes in the tumor microenvironment is limited, and their cell surface antigens are not identical to those of peripheral blood lymphocytes. Therefore, to predict the relationship between $CD8^+$ T cells and the prognosis of HNSCC, we used mIHC to detect tumor immune cell

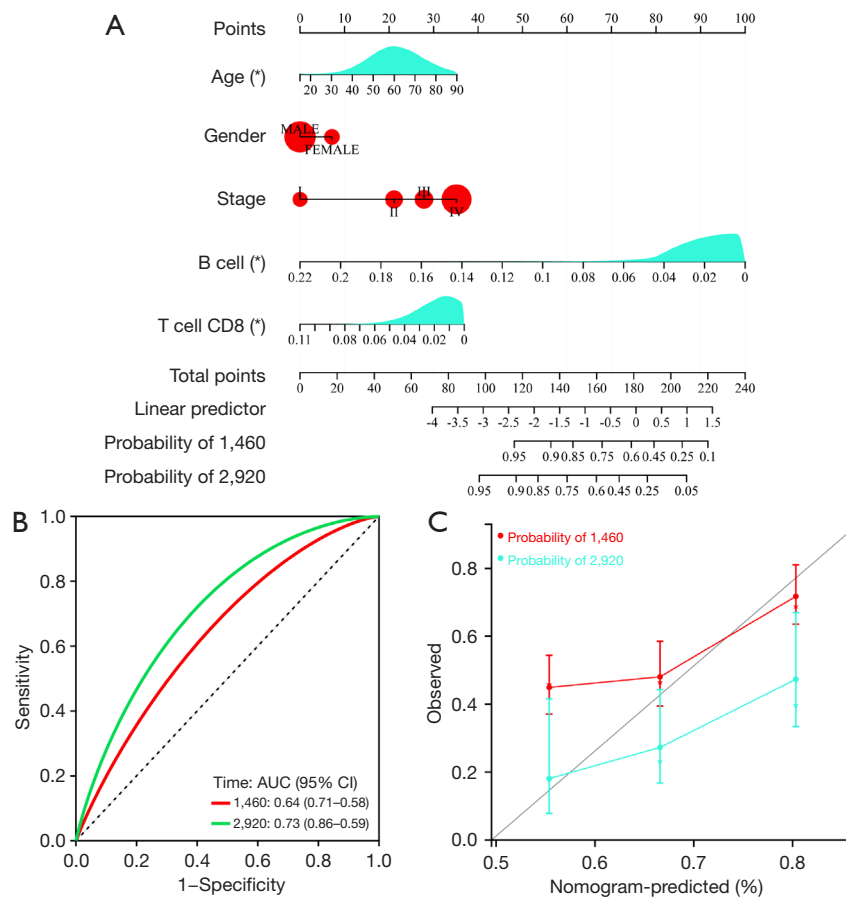


Figure 3 Accuracy and clinical applicability of the prognosis-related immune cell subpopulations. (A) A nomogram with prognosis-related immune cell subpopulations and clinicopathological features was constructed to predict the prognosis of patients with HNSCC; (B) the time-dependent ROC curves for 4- and 8-year OS predictions by the prognostic model in the TCGA-HNSCC cohort; (C) the calibration curve of the prediction model shows the degree of agreement between the predicted probability and the observed probability. The solid black line represents the perfect prediction of the ideal model, and the red and blue implementations represent the performance of the 4- and 8-year prediction models. Adjusted P values were showed as: *, $P < 0.05$. TCGA, The Cancer Genome Atlas; HNSCC, head and neck squamous cell carcinoma; ROC, receiver operating characteristic; OS, overall survival.

infiltration in 10 patients with laryngeal squamous cell carcinoma. Our multiplex immunofluorescence staining results showed infiltration of CD8⁺ T cells, NK cells, and macrophages in laryngeal cancer patients, and the three immune cells infiltrated the tumor parenchyma in higher numbers than the stroma.

In addition, we obtained information on 510 patients with HNSCC through the TCGA database including their gender, TNM stage, clinical stage, grade, and age (the median age was 60.5 years). A Cox regression model was used to determine correlation of clinicopathological factors with prognosis in HNSCC and showed age, stage IV, B cells, and CD8⁺ T cells were significantly associated with

it. Further, multivariate Cox regression analysis showed age, stage IV, B cells, and CD8⁺ T cells were significantly associated with the prognosis of HNSCC. These results demonstrate that CD8⁺ T cells are an independent prognostic factor in HNSCC patients. To further investigate the relationship between tumor immune infiltrating cells and the prognosis of HNSCC, we analyzed immune infiltration using the EPIC method and showed the results of the prognostic analysis by survival curves. Our study showed that patients with low expression of CD4⁺ T cells had a better prognosis, while those with high expression of endothelial cells, CD8 T cells, and B cells also had a better prognosis. In addition, NK cells, macrophages, and cancer-

associated fibroblasts had no significant correlation with the prognosis of HNSCC patients.

Our study has several shortcomings. First, a small sample size was used and only focused on mRNA sequencing data from TCGA, and future work will need to expand the sample size and explore other public databases. Second, as retrospective studies were used the results may be biased, and further multicenter prospective studies are urgently needed. In conclusion, our study shows that CD8⁺ T-cell exhaustion in the tumor microenvironment may be used as an independent predictive factor and can also be combined with the tumor stage to improve the accuracy of prognosis assessment in HNSCC patients.

Acknowledgments

Funding: This study was supported by grants from the National Natural Science Foundation (Nos. 82070622 and 81702419), the Key Research and Development Plan of Jiangsu Province (No. BE2020668), and the Nantong Science and Technology Project (No. MS12019013).

Footnote

Reporting Checklist: The authors have completed the TRIPOD reporting checklist. Available at <https://atm.amegroups.com/article/view/10.21037/atm-22-867/rc>

Data Sharing Statement: Available at <https://atm.amegroups.com/article/view/10.21037/atm-22-867/dss>

Conflicts of Interest: All authors have completed the ICMJE uniform disclosure form (available at <https://atm.amegroups.com/article/view/10.21037/atm-22-867/coif>). The authors have no conflicts of interest to declare.

Ethical Statement: The authors are accountable for all aspects of the work in ensuring that questions related to the accuracy or integrity of any part of the work are appropriately investigated and resolved. All procedures performed in this study involving human participants were in accordance with the Declaration of Helsinki (as revised in 2013). Informed consent was obtained from the six patients, and the Ethics Committee of Affiliated Hospital of Jiangnan University approved the study protocol (No. LS2021073).

Open Access Statement: This is an Open Access article distributed in accordance with the Creative Commons

Attribution-NonCommercial-NoDerivs 4.0 International License (CC BY-NC-ND 4.0), which permits the non-commercial replication and distribution of the article with the strict proviso that no changes or edits are made and the original work is properly cited (including links to both the formal publication through the relevant DOI and the license). See: <https://creativecommons.org/licenses/by-nc-nd/4.0/>.

References

1. Jemal A, Siegel R, Ward E, et al. Cancer statistics, 2007. *CA Cancer J Clin* 2007;57:43-66.
2. Solomon B, Young RJ, Rischin D. Head and neck squamous cell carcinoma: Genomics and emerging biomarkers for immunomodulatory cancer treatments. *Semin Cancer Biol* 2018;52:228-40.
3. Yang H, Cao Y, Li ZM, et al. The role of protein p16INK4a in non-oropharyngeal head and neck squamous cell carcinoma in Southern China. *Oncol Lett* 2018;16:6147-55.
4. Chic N, Brasó-Maristany F, Prat A. Biomarkers of immunotherapy response in breast cancer beyond PD-L1. *Breast Cancer Res Treat* 2022;191:39-49.
5. Allen CT, Judd NP, Bui JD, et al. The clinical implications of antitumor immunity in head and neck cancer. *Laryngoscope* 2012;122:144-57.
6. Dong G, Chen Z, Li ZY, et al. Hepatocyte growth factor/scatter factor-induced activation of MEK and PI3K signal pathways contributes to expression of proangiogenic cytokines interleukin-8 and vascular endothelial growth factor in head and neck squamous cell carcinoma. *Cancer Res* 2001;61:5911-8.
7. de Ruiter EJ, Ooft ML, Devriese LA, et al. The prognostic role of tumor infiltrating T-lymphocytes in squamous cell carcinoma of the head and neck: A systematic review and meta-analysis. *Oncoimmunology* 2017;6:e1356148.
8. Mandal R, Şenbabaoğlu Y, Desrichard A, et al. The head and neck cancer immune landscape and its immunotherapeutic implications. *JCI Insight* 2016;1:e89829.
9. Cózar B, Greppi M, Carpentier S, et al. Tumor-Infiltrating Natural Killer Cells. *Cancer Discov* 2021;11:34-44.
10. Myers JA, Miller JS. Exploring the NK cell platform for cancer immunotherapy. *Nat Rev Clin Oncol* 2021;18:85-100.
11. Van Allen EM, Miao D, Schilling B, et al. Genomic correlates of response to CTLA-4 blockade in metastatic melanoma. *Science* 2015;350:207-11.
12. Herbst RS, Soria JC, Kowanetz M, et al. Predictive

- correlates of response to the anti-PD-L1 antibody MPDL3280A in cancer patients. *Nature* 2014;515:563-7.
13. Liu R, Hu R, Zeng Y, et al. Tumour immune cell infiltration and survival after platinum-based chemotherapy in high-grade serous ovarian cancer subtypes: A gene expression-based computational study. *EBioMedicine* 2020;51:102602.
 14. Hou Y, Nitta H, Wei L, et al. Evaluation of Immune Reaction and PD-L1 Expression Using Multiplex Immunohistochemistry in HER2-Positive Breast Cancer: The Association With Response to Anti-HER2 Neoadjuvant Therapy. *Clin Breast Cancer* 2018;18:e237-44.
 15. You K, Park S, Ryu JM, et al. Comparison of Core Needle Biopsy and Surgical Specimens in Determining Intrinsic Biological Subtypes of Breast Cancer with Immunohistochemistry. *J Breast Cancer* 2017;20:297-303.
 16. Ressel L, Poli A. Simultaneous double labelling of routinely processed paraffin tissue sections using combined immunoperoxidase, immunofluorescence, and digital image editing. *Res Vet Sci* 2010;88:122-6.
 17. Mason DY, Micklem K, Jones M. Double immunofluorescence labelling of routinely processed paraffin sections. *J Pathol* 2000;191:452-61.
 18. Bray F, Ferlay J, Soerjomataram I, et al. Global cancer statistics 2018: GLOBOCAN estimates of incidence and mortality worldwide for 36 cancers in 185 countries. *CA Cancer J Clin* 2018;68:394-424.
 19. Tsuta K, Ishii G, Kim E, et al. Primary lung adenocarcinoma with massive lymphocyte infiltration. *Am J Clin Pathol* 2005;123:547-52.
 20. Rosenberg SA, Spiess P, Lafreniere R. A new approach to the adoptive immunotherapy of cancer with tumor-infiltrating lymphocytes. *Science* 1986;233:1318-21.
 21. Schillaci R, Salatino M, Cassataro J, et al. Immunization with murine breast cancer cells treated with antisense oligodeoxynucleotides to type I insulin-like growth factor receptor induced an antitumoral effect mediated by a CD8⁺ response involving Fas/Fas ligand cytotoxic pathway. *J Immunol* 2006;176:3426-37.
 22. Geng Y, Shao Y, He W, et al. Prognostic Role of Tumor-Infiltrating Lymphocytes in Lung Cancer: a Meta-Analysis. *Cell Physiol Biochem* 2015;37:1560-71.
- (English Language Editor: B. Draper)

Cite this article as: Zhang Y, Li L, Zheng W, Zhang L, Yao N. CD8⁺ T-cell exhaustion in the tumor microenvironment of head and neck squamous cell carcinoma determines poor prognosis. *Ann Transl Med* 2022;10(6):273. doi: 10.21037/atm-22-867